

Relation between fluctuations and efficiency at maximum power for small heat engines

Guo-Hua Xu,^{1,*} Chao Jiang,¹ Yuki Minami,¹ and Gentaro Watanabe^{1,2,†}

¹*Department of Physics and Zhejiang Institute of Modern Physics,
Zhejiang University, Hangzhou, Zhejiang 310027, China*

²*Zhejiang Province Key Laboratory of Quantum Technology and Device,
Zhejiang University, Hangzhou, Zhejiang 310027, China*

(Dated: December 1, 2022)

We study the ratio between the variances of work output and heat input, $\eta^{(2)}$, for a class of four-stroke heat engines which covers various typical cycles. Recent studies on the upper and lower bounds of $\eta^{(2)}$ are based on the quasistatic limit and the linear response regime, respectively. We extend these relations to the finite-time regime within the endoreversible approximation. We consider the ratio $\eta_{\text{MP}}^{(2)}$ at maximum power and find that the square of the Curzon-Ahlborn efficiency, η_{CA}^2 , gives a good estimate of $\eta_{\text{MP}}^{(2)}$ for the class of heat engines considered, i.e., $\eta_{\text{MP}}^{(2)} \simeq \eta_{\text{CA}}^2$. This resembles the situation where the Curzon-Ahlborn efficiency gives a good estimate of the efficiency at maximum power for various kinds of finite-time heat engines. Taking an overdamped Brownian particle in a harmonic potential as an example, we can realize such endoreversible small heat engines and give an expression of the cumulants of work output and heat input. The approximate relation $\eta_{\text{MP}}^{(2)} \simeq \eta_{\text{CA}}^2$ is verified by numerical simulations. This relation also suggests a trade-off between the efficiency and the stability of finite-time heat engines at maximum power.

I. INTRODUCTION

Relation between the work output and heat input of heat engines is an important issue in thermodynamics. If the heat engine converts the heat input Q_h from a hot heat bath to the work output W and emits heat Q_c to a cold heat bath, the performance of the engine is characterized by the efficiency,

$$\eta \equiv \frac{\langle W \rangle}{\langle Q_h \rangle}. \quad (1)$$

Here, $\langle \dots \rangle$ is the ensemble average. Suppose the temperatures of the hot and cold baths are T_h and T_c , respectively, η is upper bounded by the Carnot efficiency η_C given by $\eta_C \equiv 1 - (T_c/T_h)$.

With the development of technology in recent decades, small heat engines can be realized in the sub-micron scales [1–10]. Among them, a typical example is the experimental realization of the so-called Brownian heat engine [4–7] which consists of a Brownian particle subject to a time-dependent laser trap. For the small thermal devices, thermodynamic quantities like work, heat, and entropy production are random variables defined on individual trajectories in the phase space of working substance [11–14]. Due to their small number of degrees of freedom, such small thermal devices have large fluctuations of thermodynamic quantities [15, 16]. These fluctuations can significantly affect the performance of small heat engines. Thus, it is important to study the fluctuations of work output and heat input, which reflect the stability of small heat engines.

Concerning fluctuations of the thermodynamic quantities, the performance of small heat engines has been studied [17–30]. Several features of the fluctuations have been revealed,

such as the statistics of stochastic efficiency $\tilde{\eta} \equiv W/Q_h$ [31–37] and the thermodynamics uncertainty relation (TUR) [38–45] which is the relation between the uncertainty (relative fluctuation) of thermodynamic quantities and the entropy production. More precisely, the TUR gives a lower bound of the uncertainty $\sigma_X = (\langle X^2 \rangle - \langle X \rangle^2)/\langle X \rangle^2$ for a thermodynamic quantity X . Recently, a universal bound has been found for microscopic heat engines in the quasistatic limit [22]:

$$\eta^{(2)} \equiv \frac{\langle (\Delta W)^2 \rangle}{\langle (\Delta Q_h)^2 \rangle} \leq \eta_C^2 \quad (2)$$

with $\Delta X \equiv X - \langle X \rangle$ for $X = W$ and Q_h . The ratio $\eta^{(2)}$ is the relative fluctuation between the work output and the heat input. It is noted that the smaller $\eta^{(2)}$ gives more stable work output converting from the fluctuating heat input. Thus, $\eta^{(2)}$ reflects the stability of small heat engines.

Furthermore, recent works on $\eta^{(2)}$ also suggested its lower bound, $\eta^{(2)} \geq \eta^2$, in the linear response regime of small change in parameters [24, 46] or for a special model of the finite-time quantum Otto engine [23]. However, the relation between $\eta^{(2)}$ and η^2 for general cycles is still unclear even in the quasistatic limit. In addition, another way to interpret this lower bound is $\sigma_W \geq \sigma_{Q_h}$ which is complementary to the TURs. Therefore, the relation between $\eta^{(2)}$ and η^2 is an interesting issue for the statistics of the engine performance.

Our goal in the present work is twofold. The first one is to find a relation between $\eta^{(2)}$ and η^2 in the quasistatic limit, and the second one is to evaluate $\eta^{(2)}$ and η for the finite cycle period. For practical heat engines with nonzero power output, the discussion in the quasistatic limit is not enough. In the non-quasistatic regime, endoreversible thermodynamics made useful assumptions originally for the macroscopic irreversible heat engines (see, e.g., Refs. [47–50]). In this case, the working substance is assumed to be reversible and the irreversibility is caused solely by the irreversible heat flow between the heat bath and the working substance. Recently, the endore-

* guohuax@zju.edu.cn

† gentaro@zju.edu.cn

TABLE I. Main contents of this paper.

	section	results	Eqs. & Fig.
reversible	III A	relation between $\eta^{(2)}$ and η^2	(20) (21) (23)
	III B	lower bound of uncertainties	(34)
endoreversible	IV A	η_{MP} at maximum power	(39)
	IV B	$\eta_{MP}^{(2)}$ at maximum power	(41)
Brownian	V A	cumulant of work and heat	(66)
	V B	endoreversibility	(71)
Otto	VIA 1	η_{MP}	(90)
	VIA 2	$\eta_{MP}^{(2)}$	(94)
	VIA 3	cumulant of work	(95)
Curzon-Ahlborn	VIB 1	η_{MP}	(101)
	VIB 2	$\eta_{MP}^{(2)}$	Fig. 7

versible assumptions are generalized for the microscopic heat engines [28, 51]. For example, authors of Ref. [28] discussed the microscopic endoreversible Curzon-Ahlborn (CA) heat engine whose working substance is a highly underdamped Brownian particle. In this case, the irreversible heat exchange is caused by the interaction between the working substance and the heat bath with different temperatures.

In the framework of endoreversible thermodynamics, finite-time heat engines are usually characterized by the performance at maximum power. For example, the efficiency at maximum power (EMP), η_{MP} , is an important quantity which has been studied for various kinds of small heat engines [52–58]. Besides, the Curzon-Ahlborn efficiency, η_{CA} , gives a good estimate of η_{MP} . It is natural to ask what the fluctuation of performance at maximum power is. To answer this question, we study $\eta_{MP}^{(2)}$ at maximum power.

This paper is organized as follows. In Sec. II, we give the setup of four-stroke heat engines consisting of two adiabatic strokes and two heat transfer strokes. This setup includes various types of cycles, e.g., the Otto, Brayton, and Diesel cycles [59]. In Sec. III, we consider reversible small heat engines and assume that the heat capacities are constant in the heat transfer strokes. We discuss the relation between $\eta^{(2)}$ and η^2 , and find a lower bound of the uncertainties of work and heat. In Sec. IV, based on the endoreversible assumption, an approximate relation, $\eta_{MP}^{(2)} \simeq \eta_{CA}^2$, is proposed for endoreversible small heat engines. In Sec. V, we discuss the endoreversibility of the Brownian heat engine which consists of an overdamped Brownian particle in a harmonic potential. In Sec. VI, using the setup introduced in Sec. V, we show two examples of the endoreversible small heat engines, the Brownian Otto engine and Brownian CA engine. Our main result, $\eta_{MP}^{(2)} \simeq \eta_{CA}^2$, is examined numerically. The structure of this paper and where each result is presented are summarized in Table I.

II. SETUP

In this paper, we consider a small heat engine operating with two heat baths with the temperatures T_h and T_c ($T_h > T_c$),

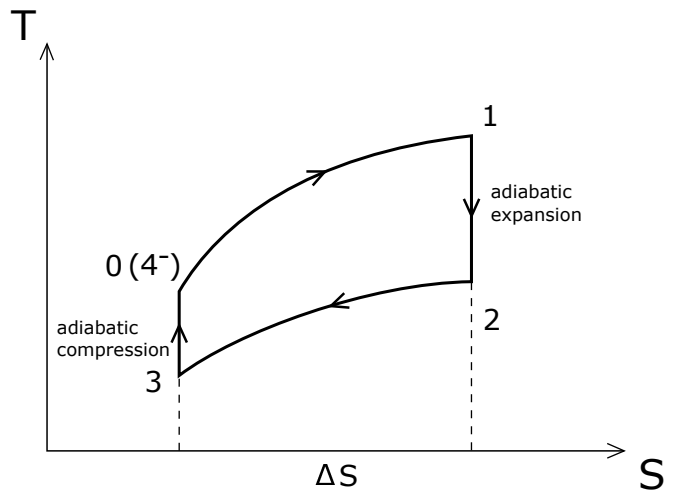


FIG. 1. T - S diagram of the class of four-stroke cycles considered in the present work. The cycles consist of two adiabatic strokes (adiabatic expansion $1 \rightarrow 2$ and adiabatic compression $3 \rightarrow 4^-$) and two heat transfer strokes ($0 \rightarrow 1$ and $2 \rightarrow 3$).

and focus on a class of four-stroke cycles consisting of two adiabatic strokes ($1 \rightarrow 2$ and $3 \rightarrow 4^-$) and two heat transfer strokes ($0 \rightarrow 1$ and $2 \rightarrow 3$). The cycle on the T - S plane is shown in Fig. 1. Here, T and S are the temperature and the entropy of the working substance, respectively. The final node 4^- of the cycle is statistically equivalent to the initial node 0, i.e., the phase space probability density function (PDF) of the working substance at these nodes are the same. During the heat transfer stroke $0 \rightarrow 1$ ($2 \rightarrow 3$), heat flows into (out of) the engine from the hot heat bath (to the cold bath). Throughout the paper, we take the sign convention where Q_h is positive when the heat is absorbed by the engine from the hot bath and Q_c is positive when the heat is emitted from the engine to the cold bath, i.e., $\langle Q_i \rangle > 0$ ($i = h$ and c).

Our goal is to derive the relation between the ratio $\eta^{(2)} \equiv \langle (\Delta W)^2 \rangle / \langle (\Delta Q_h)^2 \rangle$ and the efficiency $\eta \equiv \langle W \rangle / \langle Q_h \rangle$ for various kinds of cycles not only in the quasistatic regime but also in the finite-time regime.

III. REVERSIBLE SMALL HEAT ENGINE

In this section, we compare $\eta^{(2)}$ and η and study the uncertainties of work and heat in the reversible case [60]. We consider the working substance following a reversible cycle. The parameter change of the working substance is much slower than the relaxation, so that the working substance is always in the (local) equilibrium state during the heat transfer strokes.

We make the following three assumptions on the four-stroke small heat engines:

(i) We consider particular types of the heat transfer stroke where the amount of the heat exchange between the engine and the bath can be described by the heat capacity C_i and the temperature change dT of the working substance in the form

of

$$\langle dQ_i \rangle = |C_i dT|. \quad (3)$$

Here, $i = h$ (c) for the heat transfer stroke $0 \rightarrow 1$ ($2 \rightarrow 3$) with the hot (cold) heat bath. Such heat transfer strokes include isochoric strokes and isobaric strokes. Thus, various typical cycles such as the Otto, Diesel, and Brayton cycles are covered in the present discussion. For example, the Otto engine absorbs (emits) the heat during the hot (cold) isochoric stroke with the heat capacity C_h (C_c) at constant volume, and the Diesel engine absorbs the heat during the isobaric stroke with the heat capacity C_h at constant pressure and emits the heat during the isochoric stroke with the heat capacity C_c at constant volume.

(ii) We further assume that the heat capacity C_i of the working substance is constant (and positive) during each heat transfer stroke [61]. In addition to C_i , we assume that the heat capacity C_V at constant volume, $C_V \equiv (\partial \langle E \rangle / \partial T)_V$, is also constant during each heat transfer stroke and does not depend on the volume. Since the heat capacity C_i is positive, we always have $T_1 - T_0 > 0$ and $T_3 - T_2 < 0$. To avoid the situation in which the two heat transfer strokes cross on the T - S plane, we consider the cases with $T_1 \geq T_2$ and $T_0 \geq T_3$. If the two heat transfer strokes cross each other, the whole cycle can be decomposed into two sub-cycles with the clock-wise and counter-clock-wise directions on the T - S plane corresponding to a heat engine and a refrigerator, respectively.

(iii) We consider reversible cycles which consist of reversible heat transfer strokes and quasistatic adiabatic strokes without irreversibility at the connections between them. In the present case, the quasistatic adiabatic strokes start from a canonical state at the temperature T_{init} because the working substance is always in the equilibrium state during the preceding reversible heat transfer stroke. Since the number of degrees of freedom in the working substance of microscopic heat engines is small, the energy distribution of the working substance is generally not a canonical distribution at the end of the quasistatic adiabatic strokes. When the engine is coupled to a heat bath at the temperature T_{fin} after an adiabatic stroke, irreversible heat exchange occurs unless the working substance is already in the canonical state at T_{fin} . A necessary and sufficient condition for the initial state and the final state of the quasistatic adiabatic stroke to be canonical states at the temperature T_{init} and T_{fin} , respectively, is

$$\frac{E_{\text{init}}}{T_{\text{init}}} = \frac{E_{\text{fin}}}{T_{\text{fin}}}, \quad (4)$$

up to a constant [62]. Here, E_{init} (E_{fin}) is the internal energy of the initial (final) state of the quasistatic adiabatic stroke. Note that E_{init} and E_{fin} are random variables and Eq. (4) has to hold for each realization.

A. Relation between $\eta^{(2)}$ and η

Based on the above mentioned assumptions, we can derive the variances of work output and heat input. Work output during the quasistatic adiabatic strokes $1 \rightarrow 2$ and $3 \rightarrow 4^-$ is given

by

$$W_{1 \rightarrow 2} = E_1 - E_2 = \left(1 - \frac{T_2}{T_1}\right) E_1 \quad (5)$$

and

$$W_{3 \rightarrow 4^-} = E_3 - E_{4^-} = \left(\frac{T_3}{T_0} - 1\right) E_{4^-}, \quad (6)$$

respectively, with E_j and T_j being the internal energy and the temperature of the working substance at node j , respectively. Here, we have assumed the reversibility condition (4) for the adiabatic strokes $1 \rightarrow 2$ and $3 \rightarrow 4^-$:

$$\frac{E_1}{T_1} = \frac{E_2}{T_2} \quad \text{and} \quad \frac{E_3}{T_3} = \frac{E_{4^-}}{T_0}. \quad (7)$$

In the quasistatic limit, fluctuations of work during the heat transfer strokes $0 \rightarrow 1$ and $2 \rightarrow 3$ are negligible due to the same reason for quasistatic isothermal processes [11, 22, 42]:

$$\Delta W_{0 \rightarrow 1} \equiv W_{0 \rightarrow 1} - \langle W_{0 \rightarrow 1} \rangle \simeq 0 \quad (8)$$

and

$$\Delta W_{2 \rightarrow 3} \equiv W_{2 \rightarrow 3} - \langle W_{2 \rightarrow 3} \rangle \simeq 0. \quad (9)$$

In addition, since the quasistatic adiabatic strokes $1 \rightarrow 2$ and $3 \rightarrow 4^-$ are separated by a reversible heat transfer stroke, their work output $W_{1 \rightarrow 2}$ and $W_{3 \rightarrow 4^-}$ are not correlated. Therefore, the variance of work output in one cycle is given by the sum of the variances in the uncorrelated quasistatic adiabatic strokes:

$$\begin{aligned} \langle (\Delta W)^2 \rangle &= \langle (\Delta W_{1 \rightarrow 2})^2 \rangle + \langle (\Delta W_{3 \rightarrow 4^-})^2 \rangle \\ &= \left(1 - \frac{T_2}{T_1}\right)^2 \langle (\Delta E_1)^2 \rangle + \left(1 - \frac{T_3}{T_0}\right)^2 \langle (\Delta E_0)^2 \rangle \\ &= k_B C_V [(T_1 - T_2)^2 + (T_0 - T_3)^2]. \end{aligned} \quad (10)$$

Here, we have used the property: $\langle (\Delta E_j)^2 \rangle = k_B C_V T_j^2$ [63].

Heat absorbed from the hot bath during the heat transfer stroke $0 \rightarrow 1$ reads

$$Q_h = E_1 - E_0 - W_{0 \rightarrow 1}, \quad (11)$$

and its variance is given by

$$\langle (\Delta Q_h)^2 \rangle = \langle (\Delta E_0)^2 \rangle + \langle (\Delta E_1)^2 \rangle \quad (12)$$

$$= k_B C_V (T_1^2 + T_0^2) \quad (13)$$

because E_0 and E_1 are uncorrelated and $\Delta W_{0 \rightarrow 1} \simeq 0$. Thus, from Eqs. (10) and (13), the ratio $\eta^{(2)}$ can be written as

$$\eta^{(2)} = \frac{\langle (\Delta W)^2 \rangle}{\langle (\Delta Q_h)^2 \rangle} = \frac{(T_1 - T_2)^2 + (T_0 - T_3)^2}{T_1^2 + T_0^2}. \quad (14)$$

For the reversible cycle, the temperatures $\{T_j\}$ of the working substance are not independent. The mean value of the entropy change of the working substance during the heat absorption or the heat emission stroke is given by

$$\Delta S_i = (-1)^{j/2} \int_j^{j+1} \frac{\langle dQ_i \rangle}{T} = C_i \ln \frac{T_{j+1}}{T_j}, \quad (15)$$

where $j = 0$ for $i = h$ and $j = 2$ for $i = c$. Since the cycle is closed, the mean value of the net entropy change over the cycle is zero:

$$\Delta S_h + \Delta S_c = C_h \ln \frac{T_1}{T_0} + C_c \ln \frac{T_3}{T_2} = 0. \quad (16)$$

Thus, we obtain

$$\tilde{t}^\theta = T_3/T_2, \quad (17)$$

where $\tilde{t} \equiv T_0/T_1$ is the temperature ratio with $0 < \tilde{t} < 1$ and $\theta \equiv C_h/C_c$ is the heat capacity ratio with $\theta > 0$.

The working substance is in local equilibrium with temperature $T_c < T < T_h$, as assumed in endoreversible thermodynamics. In the whole cycle, the maximum (minimum) temperature of the working substance is T_1 (T_3). Since the durations of the heat transfer strokes are sufficiently long, we have $T_1 = T_h$ and $T_3 = T_c$. Then, the Carnot efficiency is given by

$$\eta_C = 1 - \frac{T_3}{T_1}. \quad (18)$$

Now, we can express $\eta^{(2)}$ and η with three parameters: θ , \tilde{t} , and η_C . The efficiency is given by

$$\eta = 1 - \frac{\langle Q_c \rangle}{\langle Q_h \rangle} = 1 - \frac{T_2 - T_3}{\theta(T_1 - T_0)}. \quad (19)$$

Substituting Eqs. (17) and (18) into Eq. (19), we get

$$\eta = 1 - \frac{(1 - \eta_C)(1 - \tilde{t}^\theta)}{\theta(1 - \tilde{t})\tilde{t}^\theta}, \quad (20)$$

and substituting Eqs. (17) and (18) into Eqs. (14), we get

$$\eta^{(2)} = \left(1 - \frac{1 - \eta_C}{\tilde{t}^\theta}\right)^2 \frac{1}{1 + \tilde{t}^2} + \left(1 - \frac{1 - \eta_C}{\tilde{t}}\right)^2 \frac{\tilde{t}^2}{1 + \tilde{t}^2}. \quad (21)$$

Since $0 < \tilde{t} < 1$ and $\theta > 0$, $\eta^{(2)}$ is upper bounded by η_C^2 :

$$\eta^{(2)} < \eta_C^2, \quad (22)$$

which is consistent with the universal bound on $\eta^{(2)}$ proven for general quasistatic cycles in our previous work [22]. It is interesting to note that, although the present discussion leading to Eq. (21) does not include the Carnot cycle, the resulting Eq. (21) for $\tilde{t} = 1$ and $\theta = 1$ is consistent with $\eta^{(2)}$ of the Carnot cycle, $\eta^{(2)} = \eta_C^2$, obtained in Ref. [22].

Next, we compare the values of $\eta^{(2)}$ and η^2 . For $\theta = 1$, which means that the two heat transfer strokes in the cycle are the same type (e.g., the Otto cycle and the Brayton cycle), we readily get

$$\eta^{(2)} = \eta^2 \quad (23)$$

from Eqs. (20) and (21) with

$$\eta = 1 - \frac{T_3}{T_0} = 1 - \frac{T_2}{T_1}. \quad (24)$$

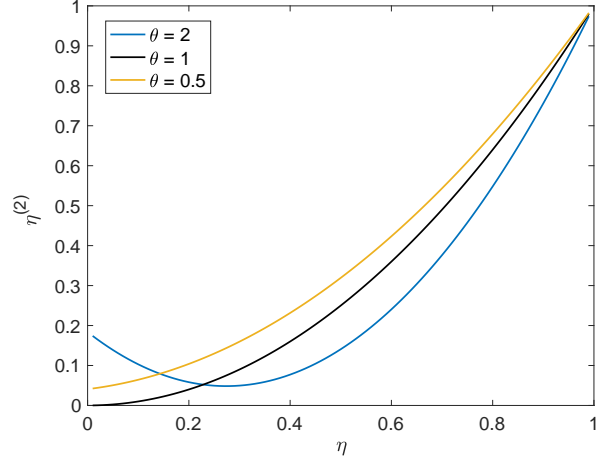


FIG. 2. $\eta^{(2)}$ as a function of η for $\theta = 0.5, 1$, and 2 . Here, we set $\tilde{t} = 0.4$. The black line ($\eta^{(2)}$ for $\theta = 1$) shows $\eta^{(2)} = \eta^2$.

For $\theta \neq 1$, as shown in Fig. 2, $\eta^{(2)}$ is a shifted quadratic function of η . For $0 < \theta < 1$, we have

$$\eta^{(2)} > \eta^2, \quad (25)$$

which is consistent with the lower bound in the linear response regime of small change in parameters [24, 46]. However, for $\theta > 1$, η^2 does not give the lower bound of $\eta^{(2)}$ any more, and $\eta^{(2)}$ could be larger or smaller than η^2 . This result can also be interpreted as the relation between uncertainties σ_W and σ_{Q_h} of the work output and the heat input from the hot heat bath, which are defined as $\sigma_X = (\langle X^2 \rangle - \langle X \rangle^2) / \langle X \rangle^2$ with $X = W$ and Q_h . We have

$$\sigma_W = \sigma_{Q_h} \quad (26)$$

when $\theta = 1$, and

$$\sigma_W > \sigma_{Q_h} \quad (27)$$

when $0 < \theta < 1$. σ_W could be larger or smaller than σ_{Q_h} when $\theta > 1$.

B. Uncertainties of work output and heat input

Now, we evaluate the uncertainties of work output and heat input and give a lower bound of them. Before discussing the four-stroke cycles with constant C_i , let us first consider the Carnot cycle as a simple example which gives $\eta^{(2)} = \eta_C^2$ and $\sigma_W = \sigma_{Q_h}$ [22]. In this case, we have $\langle (\Delta Q_h)^2 \rangle = 2k_B C_V T_h^2$ and $\langle Q_h \rangle = T_h \Delta S$ with $\Delta S \equiv \Delta S_h = -\Delta S_c > 0$, and the uncertainty σ_{Q_h} is given by

$$\sigma_{Q_h} = \frac{\langle (\Delta Q_h)^2 \rangle}{\langle Q_h \rangle^2} = \frac{2k_B C_V}{(\Delta S)^2}. \quad (28)$$

The Carnot engine whose working substance is an overdamped Brownian particle trapped in the potential $U =$

$kx^{2n}/2n$ (n is a natural number) discussed in Ref. [42] is a special case of Eq. (28) [64].

Next, let us go back to the reversible four-stroke cycles with constant C_i in the heat transfer strokes $0 \rightarrow 1$ and $2 \rightarrow 3$. According to Eqs. (3) and (13), the mean value of the absorbed heat from the hot heat bath is given by $\langle Q_h \rangle = C_h(T_1 - T_0)$, and its variance is given by $\langle (\Delta Q_h)^2 \rangle = k_B C_V (T_1^2 + T_0^2)$. Thus, we get

$$\sigma_{Q_h} = \frac{k_B C_V}{C_h^2} \frac{1 + \tilde{t}^2}{(1 - \tilde{t})^2}, \quad (29)$$

and see that σ_{Q_h} is a function of the temperature ratio $\tilde{t} = T_0/T_1$ which is related to the change ΔS of the entropy:

$$\tilde{t} = \exp(-\Delta S/C_h). \quad (30)$$

In the same way, we have

$$\sigma_{Q_c} = (k_B C_V / C_c^2) (T_2^2 + T_3^2) (T_2 - T_3)^{-2} \quad (31)$$

which depends on the temperature ratio T_2/T_3 with

$$T_2/T_3 = \exp(\Delta S/C_c). \quad (32)$$

From Eqs. (29), (30), (31), and (32), we obtain the uncertainty of the absorbed/emitted heat σ_{Q_i} ($i = h, c$) and find its lower bound given by

$$\sigma_{Q_i} = \frac{k_B C_V}{2C_i^2} \frac{\cosh(\Delta S/C_i)}{\sinh^2[\Delta S/(2C_i)]} \geq \frac{2k_B C_V}{(\Delta S)^2}. \quad (33)$$

For $0 < \theta \leq 1$, from Eq. (27), we have $\sigma_W \geq \sigma_{Q_h} \geq 2k_B C_V / (\Delta S)^2$, where the first equality is satisfied when $\theta = 1$ and the second equality is satisfied when $\Delta S \ll C_h$. For $\theta > 1$, σ_W could be larger or smaller than σ_{Q_h} but has the same lower bound. In conclusion, we have

$$\sigma_{Q_i} \geq \frac{2k_B C_V}{(\Delta S)^2} \quad \text{and} \quad \sigma_W \geq \frac{2k_B C_V}{(\Delta S)^2}. \quad (34)$$

This lower bound is given by the uncertainty of work output and absorbed/emitted heat in the corresponding Carnot cycle with the same value of ΔS .

IV. ENDOREVERSIBLE SMALL HEAT ENGINE

In this section, we consider the small heat engine operating in a finite cycle period τ which satisfies the endoreversible assumptions. To show a subtle difference between the endoreversible assumptions in the microscopic and macroscopic systems, we first introduce endoreversible thermodynamics for macroscopic engines before giving our main result for the endoreversible small heat engines. At the end of this section, we derive $\eta_{MP} = \eta_{CA}$ [Eq. (39)] for a particular class of small heat engines, such that the two heat transfer strokes are the same type, i.e., $\theta = 1$, with the constant heat capacities and heat conductivities.

A. Endoreversible thermodynamics for macroscopic engines

In endoreversible thermodynamics, we assume that the irreversibility is caused solely by the irreversible heat transfer between the engine and the bath, and the other processes are reversible [49, 50]. For macroscopic endoreversible engines, we assume that the relaxation time of the working substance is much shorter than the timescale of the parameter change. Thus, the working substance is in local equilibrium with an internal temperature T_{in} . This internal temperature is generally different from the temperature of the baths. In addition, the adiabatic strokes are assumed to be reversible but operated in a short time compared with the cycle period. The working substance follows a reversible cycle, and the mean value of the entropy production Σ should be zero:

$$\Sigma \equiv \Delta S - \left\langle \int_0^\tau \frac{\dot{Q}}{T_{in}} dt \right\rangle = 0. \quad (35)$$

Here, ΔS is the change of the entropy in the working substance through one cycle, which is zero for the engine running periodically. For small heat engines, we consider the same assumption of endoreversibility but from a different microscopic mechanism.

For macroscopic engines, there is usually an intermediate heat conducting medium between the working substance and the bath during the heat transfer strokes. Due to the finite heat flow and the finite duration of the heat transfer strokes, there is a temperature difference between the bath and the working substance. The mean value of the heat flow between the bath and the working substance is assumed to be proportional to the temperature difference between them (i.e., the Fourier or the Newton law). Since we consider sufficiently large timescale such that the heat flow has already reached a steady state, the average heat flux from the bath to the heat conducting medium and that from the heat conducting medium to the working substance are in balance. Therefore, within this formalism, we ignore the presence of nonzero mean value of the energy stored in the heat conducting medium. Furthermore, in the standard setup of the small heat engines, there is no intermediate heat conducting medium as we will discuss later.

If the working substance follows the Carnot cycle and the heat transfer follows the Newton law, the engine is referred to as the Curzon-Ahlborn heat engine [48]. The internal temperatures T_{ih} and T_{ic} during the hot and cold isothermal strokes give the efficiency of the Carnot engine as $\eta = 1 - (T_{ic}/T_{ih})$. According to the Newton law, the mean value of heat absorbed from the hot heat bath is given by

$$\langle Q_h \rangle = \alpha_h \tau_h (T_h - T_{ih}) \quad (36)$$

with the conductivity α_h and the duration τ_h of the hot isothermal stroke, and the mean value of heat emitted to the cold heat bath with the duration τ_c and the conductivity α_c is given by $\langle Q_c \rangle = \alpha_c \tau_c (T_{ic} - T_c)$. To maximize the power under given conductivities (α_h and α_c) and bath temperatures (T_h and T_c), we optimize the internal temperatures (T_{ih} and T_{ic}) and the durations (τ_h and τ_c). Then, we obtain the optimum condition

for T_{ih} and T_{ic} (see, e.g., Ref. [49] for detailed derivation):

$$\frac{T_{ic}^*}{T_{ih}^*} = \sqrt{\frac{T_c}{T_h}}, \quad (37)$$

where T_{ih}^* and T_{ic}^* are the optimum values of T_{ih} and T_{ic} . Therefore, the efficiency at maximum power η_{CA} of the CA engine is given by [49]

$$\eta_{CA} = 1 - \sqrt{\frac{T_c}{T_h}}. \quad (38)$$

In the present paper, we consider not only the CA engines but also the class of four-stroke heat engines introduced in the previous section. In the latter case, during each heat transfer stroke, the internal temperature changes while the bath temperatures T_h and T_c are constant, and the heat transfer follows the Fourier law. Following the derivation in Ref. [55], we find that, if the two heat transfer strokes in the cycle are the same type ($\theta = 1$, e.g., the Otto cycle and the Brayton cycle), the efficiency η_{MP} at maximum power is given by

$$\eta_{MP} = \eta_{CA}. \quad (39)$$

We also obtain this result for the endoreversible small heat engines with constant conductivities α_c and α_h . The detailed derivation is shown at the end of this section.

B. Endoreversible thermodynamics for small heat engines

Now, we consider endoreversible small heat engines. We assume a special class of working substance such that its energy distribution is always given by the canonical distribution function with the effective temperature \tilde{T} even if the working substance is far from equilibrium with the heat bath in the irreversible heat transfer strokes. It is noted that the effective temperature \tilde{T} is generally different from the bath temperature. We also assume direct heat transfer between the working substance and the heat bath, and there is no heat conducting medium between them. This situation is possible when the particles in the bath directly interact with the particles of the working substance such as Brownian heat engines [4, 5, 7, 52] and the interaction between them is sufficiently weak. This situation can also be realized in an endoreversible quantum Otto cycle [51]. Similarly to macroscopic endoreversible thermodynamics, we assume that the adiabatic strokes are reversible and the irreversibility is caused solely by the heat flow due to the difference between \tilde{T} and the bath temperature. If the mean value of the heat transfer is linear with respect to the temperature difference, one can reproduce the CA efficiency for the engine operating in the Carnot cycle. One example of microscopic CA engines has been discussed in Ref. [28] which considers a highly underdamped Brownian particle as the working substance.

In our work, we study the fluctuation ratio $\eta_{MP}^{(2)}$ at maximum power for endoreversible small heat engines. In the quasistatic limit, as discussed in Sec. III, the fluctuations of work and heat depend solely on the energy fluctuation at each node,

and the correlations of work and heat in each stroke are negligible. If the cycle period at maximum power is sufficiently large, the discussion in Sec. III is still applicable. In addition, since there is no heat conducting medium between the working substance and the bath, fluctuation of heat input to the working substance is exactly equal to fluctuation of heat output from the bath. Then, our result Eq. (23) holds and the ratio $\eta_{MP}^{(2)}$ at maximum power is given by $\eta_{MP}^{(2)} = \eta_{MP}^2$. Substituting Eq. (39) into Eq. (23), we have

$$\eta_{MP}^{(2)} = \eta_{CA}^2 = \left(1 - \sqrt{\frac{T_c}{T_h}}\right)^2. \quad (40)$$

It is noted that Eq. (40) is obtained for large cycle period and constant heat conductivities. For more general cases, our result Eq. (40) may not be valid. However, as verified for a microscopic model in the next section, the following approximate relation still holds for various kinds of endoreversible small heat engines:

$$\eta_{MP}^{(2)} \simeq \eta_{CA}^2, \quad (41)$$

i.e., η_{CA}^2 gives a good estimate of $\eta_{MP}^{(2)}$. This resembles the situation where the CA efficiency gives a good estimate of the efficiency at maximum power. Although η_{MP} is not always equal to η_{CA} , the approximate relation

$$\eta_{MP} \simeq \eta_{CA} \quad (42)$$

holds for various kinds of heat engines with reasonable choices of optimization conditions. Similarly, we find that $\eta_{MP}^{(2)} \simeq \eta_{CA}^2$ holds for a wide class of finite-time heat engines with large cycle period. In the next section, we will show that the approximate relation $\eta_{MP}^{(2)} \simeq \eta_{CA}^2$ is applicable to the endoreversible small heat engines even when the cycle period is very small compare to the correlation time of work and heat.

C. Derivation of Eq. (39)

Finally, we give a derivation of Eq. (39) for the four-stroke heat engines with constant heat capacity $C \equiv C_h = C_c$. In this case, the mean value of work output in one cycle is given by

$$\langle W \rangle = \langle Q_h \rangle - \langle Q_c \rangle = C(\tilde{T}_1 - \tilde{T}_0 - \tilde{T}_2 + \tilde{T}_3), \quad (43)$$

where \tilde{T}_j is the effective temperature at node j , and the cycle period is defined by

$$\tau = \gamma(\tau_h + \tau_c), \quad (44)$$

where τ_h and τ_c are the duration of heat transfer strokes and γ is the ratio of the cycle period to the duration of the heat transfer strokes. (In the usual analysis of endoreversible thermodynamics, where the duration of the adiabatic strokes is assumed to be much shorter than that of the heat transfer strokes, γ is set to unity as we shall do later.) Then the power $P = \langle W \rangle / \tau$

depends on $\{\tilde{T}_j\}$, τ_h , and τ_c . We maximize the power by optimizing $\{\tilde{T}_j\}$, τ_h , and τ_c under given T_h , T_c , α_h , and α_c . According to the Fourier law, the mean value of the heat flow \dot{Q}_i for $i = h$ and c is given by

$$\langle \dot{Q}_i \rangle = \alpha_i (T_i - \tilde{T}). \quad (45)$$

The time evolution of \tilde{T} during each heat transfer stroke follows the differential equation:

$$\frac{d\tilde{T}(t)}{dt} = \alpha_i (\tilde{T}(t) - T_i) / C. \quad (46)$$

For the stroke $0 \rightarrow 1$, the solution is

$$\tilde{T}_1 - T_h = (\tilde{T}_0 - T_h) \exp(-\alpha_h \tau_h / C), \quad (47)$$

and for the stroke $2 \rightarrow 3$, the solution is

$$\tilde{T}_3 - T_c = (\tilde{T}_2 - T_c) \exp(-\alpha_c \tau_c / C). \quad (48)$$

Since the working substance follows the reversible cycle, as Eq. (35), the relation between \tilde{T}_j and η is the same as Eq. (24) in the quasistatic limit discussed in Sec. III. For $\theta = 1$, we have

$$\eta = 1 - \frac{\tilde{T}_3}{\tilde{T}_0} = 1 - \frac{\tilde{T}_2}{\tilde{T}_1}. \quad (49)$$

Then, from Eqs. (47), (48), and (49), we have four equations for the four variables $\{\tilde{T}_j\}$. Thus, \tilde{T}_j is a function of the efficiency and the durations τ_h and τ_c , i.e.,

$$\tilde{T}_j = \tilde{T}_j(\eta, \tau_h, \tau_c; T_h, T_c, \alpha_h, \alpha_c). \quad (50)$$

Therefore, optimizing $\{\tilde{T}_j\}$, τ_h , and τ_c under the constraints of Eqs. (47), (48), and (49) is equivalent to optimizing η , τ_h , and τ_c with the same constraints. The power is given by

$$P = \frac{\langle W \rangle}{\tau} = \frac{2C\eta[(1-\eta)T_h - T_c]}{\gamma(1-\eta)(\tau_h + \tau_c)} \frac{\sinh\left(\frac{\alpha_c \tau_c}{2C}\right) \sinh\left(\frac{\alpha_h \tau_h}{2C}\right)}{\sinh\left(\frac{\alpha_c \tau_c}{2C} + \frac{\alpha_h \tau_h}{2C}\right)}, \quad (51)$$

which can be separated into a product of the following two functions:

$$f_1(\eta; T_h, T_c) = \frac{2C\eta[(1-\eta)T_h - T_c]}{\gamma(1-\eta)} \quad (52)$$

and

$$f_2(\tau_h, \tau_c; T_h, T_c, \alpha_h, \alpha_c) = \frac{\sinh\left(\frac{\alpha_c \tau_c}{2C}\right) \sinh\left(\frac{\alpha_h \tau_h}{2C}\right)}{(\tau_h + \tau_c) \sinh\left(\frac{\alpha_c \tau_c}{2C} + \frac{\alpha_h \tau_h}{2C}\right)}. \quad (53)$$

When the power is maximized, we have

$$\left(\frac{\partial f_1}{\partial \eta}\right)_{\{T_i\}} = \left(\frac{\partial f_2}{\partial \tau_h}\right)_{\{T_i\}, \{\alpha_i\}} = \left(\frac{\partial f_2}{\partial \tau_c}\right)_{\{T_i\}, \{\alpha_i\}} = 0. \quad (54)$$

η only depends on $(\partial f_1 / \partial \eta)_{\{T_i\}} = 0$, and the solution leads to

$$\eta_{\text{MP}} = 1 - \sqrt{\frac{T_c}{T_h}}. \quad (55)$$

It is worth noting that, as shown in the next section, even if the conductivities α_c and α_h depend on the driving protocols, our results Eqs. (41) and (42) can still give a good estimate for $\eta_{\text{MP}}^{(2)}$ and η_{MP} .

V. BROWNIAN HEAT ENGINE

In this section, we discuss the endoreversible Brownian heat engine which consists of an overdamped Brownian particle trapped in a time-dependent harmonic oscillator potential. We first introduce the Brownian heat engine and give an expression of the cumulants of work output and heat input. Then, we show that the Brownian heat engine satisfies the endoreversible approximation and is compatible with the linear heat transfer laws.

A. Statistics of work and heat

The Hamiltonian of the working substance in the Brownian heat engine is given by

$$H(x, t) = V(x, t) = \frac{1}{2} \lambda(t) x^2, \quad (56)$$

where x is the position of the Brownian particle and $\lambda(t)$ is the stiffness of the potential which can be controlled externally. There are two external control parameters in our system, $\lambda(t)$ and the water temperature $T(t)$, and they are changed cyclically with the cycle period τ : $\lambda(t + \tau) = \lambda(t)$ and $T(t + \tau) = T(t)$.

The time evolution of the phase-space PDF $p(x, t)$ is given by the following Fokker-Planck equation [12]:

$$\partial_t p(x, t) = \mu \{ \partial_x [(\partial_x V) p] + k_B T \partial_x^2 p \}, \quad (57)$$

where μ is the mobility of the Brownian particle. When the engine is stable, the PDF is also periodic in time with the period τ : $p(x, t) = p(x, t + \tau)$. Such a periodic solution of Eq. (57) is [52]

$$p(x, t) = \frac{1}{\sqrt{2\pi\sigma_x(t)}} \exp\left\{-\frac{x^2}{2\sigma_x(t)}\right\} \quad (58)$$

with $\langle x(t) \rangle = 0$ and $\sigma_x(t) \equiv \langle (x - \langle x \rangle)^2 \rangle = \langle x^2(t) \rangle$ whose equation of motion is given by

$$\dot{\sigma}_x = -2\mu \lambda \sigma_x + 2\mu k_B T. \quad (59)$$

Here, the dot represents the derivative with respect to time. In this model, the correlation function $\phi(t_1, t_2) \equiv \langle x(t_1)x(t_2) \rangle$ is

analytically solvable [65], and the solution is given by

$$\begin{aligned} \phi(t_1, t_2) &= e^{-[f(t_1)+f(t_2)]} 2\mu \\ &\times \left(\int_0^{\min(t_1, t_2)} e^{2f(t)} T(t) dt + \frac{\int_0^\tau e^{2f(t)} T(t) dt}{e^{2f(\tau)} - 1} \right) \end{aligned} \quad (60)$$

with $f(t) \equiv \mu \int_0^t dt' \lambda(t')$.

The work output through one cycle is given by

$$\begin{aligned} W[x(t)|_0^\tau] &= - \int_0^\tau \frac{\partial V(x, t)}{\partial \lambda} \dot{\lambda}(t) dt \\ &= - \int_0^\tau x^2(t) \frac{\dot{\lambda}(t)}{2} dt. \end{aligned} \quad (61)$$

The mean value of work in an infinitesimal time interval dt is given by

$$\langle dW \rangle = -\sigma_x(t) \dot{\lambda}(t) dt / 2. \quad (62)$$

During the heat transfer stroke $0 \rightarrow 1$ from t_0 to t_1 , the amount of heat flowing into the engine from the hot heat bath is given by

$$\begin{aligned} Q_h[x(t)|_{t_0}^{t_1}] &= V(x, t_1) - V(x, t_0) + W[x(t)|_{t_0}^{t_1}] \\ &= \int_{t_0}^{t_1} dt x^2(t) \left(\delta(t - t_1) - \delta(t - t_0) - \frac{1}{2} \partial_t \right) \lambda(t). \end{aligned} \quad (63)$$

From Eq. (62) and the first law of thermodynamics, $\langle \dot{H} \rangle = \langle \dot{Q} \rangle - \langle \dot{W} \rangle$, the mean value of the heat transfer rate is given by

$$\langle \dot{Q} \rangle = \dot{\sigma}_x(t) \lambda(t) / 2. \quad (64)$$

The work output W and the heat input Q_h are the same functional form as

$$\zeta_v[x(t)|_0^\tau] = \int_0^\tau dt \frac{K_v(t)}{2} x^2(t) \quad (65)$$

with $v = 1$ for W and $v = 2$ for Q_h . We have $K_1(t) = -\dot{\lambda}(t)$ and $K_2(t) = [\delta(t - t_1) - \delta(t - t_0) - u(t) \partial_t] \lambda(t)$, where $u(t) = 1$ when $t_0 < t < t_1$ and $u(t) = 0$ otherwise. Since $x(t)$ is a Gaussian process, we can calculate the n th order cumulant $\langle \zeta_v^n \rangle_c$ ($n > 1$) using Wick's theorem, and obtain

$$\begin{aligned} \langle \zeta_v^n \rangle_c &= \frac{(n-1)!}{2} \int dt_1 K_v(t_1) \int dt_2 K_v(t_2) \dots \\ &\times \int dt_n K_v(t_n) \prod_{i=1}^{n-1} \phi(t_i, t_{i+1}) \phi(t_n, t_1). \end{aligned} \quad (66)$$

For example, the variance (i.e., the second order cumulant with $n = 2$) of work output $W_{t_0}^{(N)}$ in N cycles from t_0 to $t_0 + N\tau$ is given by

$$\langle (\Delta W_{t_0}^{(N)})^2 \rangle = \frac{1}{2} \int_{t_0}^{N\tau+t_0} dt_1 \dot{\lambda}(t_1) \int_{t_0}^{N\tau+t_0} dt_2 \dot{\lambda}(t_2) \phi^2(t_1, t_2). \quad (67)$$

Generally speaking, the cumulants of work and heat in finite number of cycles depend on the starting point. The starting-point dependence becomes negligible in the quasistatic case,

or when the number of cycles N of the operation is infinite. Furthermore, for finite τ , since the correlations of work and heat between two different cycles are non-negligible, work and heat fluctuations in infinite cycles can be very different from those in a single cycle [66]. In the present paper, we consider the fluctuations for the latter case.

B. Endoreversibility of the Brownian heat engines

Now, we discuss the endoreversibility of the Brownian heat engines. We still consider the four-stroke cycles consisting of two heat transfer strokes and two adiabatic strokes. During each adiabatic stroke, the Shannon entropy $S = -k_B \langle \ln p \rangle$ does not change. One way to realize such adiabatic strokes without heat exchange ($Q = 0$) is quenching T and λ simultaneously [52]. Such adiabatic strokes can be implemented in the current experiments. For example, in the experiment of Ref. [5], the heat engine consists of a charged Brownian particle whose λ is controlled by tuning the intensity of the trapping laser and T is controlled by applying a noisy electric force to the charged Brownian particle. Therefore, λ and T can be changed very fast compared to the timescale of the heat exchange between the bath and the working substance.

Since the PDF of the overdamped Brownian particle in our system is always in the canonical distribution given by Eq. (58), we can define the effective temperature \tilde{T} by the width of the PDF as [52]

$$k_B \tilde{T}(t) = \lambda(t) \sigma_x(t). \quad (68)$$

Thus, the heat capacity defined by the effective temperature is constant:

$$C_V = \left\langle \left(\frac{\partial H}{\partial \tilde{T}} \right)_\lambda \right\rangle = \frac{k_B}{2}. \quad (69)$$

From Eqs. (59), (64), and (68), we get the heat transfer rate as

$$\langle \dot{Q} \rangle = \frac{1}{2} \lambda \dot{\sigma}_x(t) = \mu \lambda k_B (T - \tilde{T}). \quad (70)$$

Since the Shannon entropy $S = -k_B \langle \ln p \rangle$ does not change after a cycle, the entropy production Σ per cycle defined in Eq. (35) becomes

$$\Sigma = - \left\langle \int_0^\tau \frac{\dot{Q}}{\tilde{T}} dt \right\rangle = - \frac{1}{2} \oint d \ln \sigma_x = 0. \quad (71)$$

Therefore, this model satisfies the endoreversible assumption.

According to Eq. (70), there are two ways to satisfy the linear heat transfer law. In the first way, the control parameter λ is fixed during the heat transfer strokes as in the Otto cycle, which gives the Fourier law:

$$\langle \dot{Q} \rangle = \alpha (T - \tilde{T}), \quad (72)$$

where $\alpha = k_B \mu \lambda$ is the thermal conductivity. In the second way, \tilde{T} is fixed during the heat transfer strokes as in the

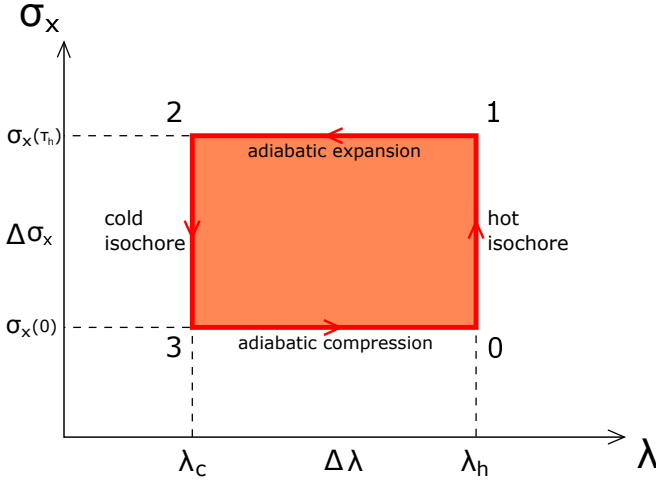


FIG. 3. Otto cycle in the σ_x - λ plane.

Curzon-Ahlborn heat engine [28], which gives the Newton law:

$$\langle Q \rangle = \alpha \tau (T - \tilde{T}), \quad (73)$$

where $\alpha = (k_B \mu / \tau) \int_0^\tau \lambda(t) dt$ is the time-averaged thermal conductivity. Using the above two ways of the control protocol in our model, we can construct the small Otto and Curzon-Ahlborn engines under the endoreversible condition. In the following, we shall discuss the two examples in detail.

VI. EXAMPLES

In this section, we discuss the Brownian Otto engine and Brownian CA engine as examples and examine our main results, the approximate relations (41) and (42). For the both cases, we first derive the maximum power and the efficiency η_{MP} under a specific constraint condition. Then, we calculate $\eta_{\text{MP}}^{(2)}$ and discuss the relation between η_{MP} , $\eta_{\text{MP}}^{(2)}$, and η_{CA} . In addition, for the Brownian Otto engine, we obtain analytical expressions of the cumulant and PDF of work.

A. Brownian Otto engine

First, we introduce the Brownian Otto engine which consists of two isochoric and two adiabatic strokes. During the hot (cold) isochoric stroke, the temperature T of the bath and the parameter λ are fixed at T_h and λ_h (T_c and λ_c), respectively, for the duration τ_h (τ_c) with $\lambda_c < \lambda_h$. In the adiabatic strokes, T and λ are quenched simultaneously in a way such that the Shannon entropy of the working substance is unchanged [52]. We define the time t_j of node j as $t_0 = 0$, $t_1 = t_2 = \tau_h$, and $t_3 = t_4 = \tau = \tau_c + \tau_h$. As shown in Fig. 3, since the variance σ_x of the position of the particle does not change during the adiabatic jumps and λ is constant during the isochoric strokes, the cycle is a rectangle in the σ_x - λ plane. From Eq. (68), we have the effective temperature \tilde{T}_j at node j as $\tilde{T}_0 = \lambda_h \sigma_x(0)$,

$\tilde{T}_1 = \lambda_h \sigma_x(\tau_h)$, $\tilde{T}_2 = \lambda_c \sigma_x(\tau_h)$, and $\tilde{T}_3 = \lambda_c \sigma_x(\tau) = \lambda_c \sigma_x(0)$. For this microscopic endoreversible Otto engine, according to Eq. (49), we have the efficiency:

$$\eta = 1 - \frac{\tilde{T}_3}{\tilde{T}_0} = 1 - \frac{\lambda_c}{\lambda_h}, \quad (74)$$

which is determined solely by the ratio λ_c/λ_h .

1. Maximum power and efficiency

Now, we derive the maximum power P_{max} and the efficiency η_{MP} . It is noted that, for the Otto engine, if the thermal conductivities α_h and α_c are constant, we have $\eta_{\text{MP}} = \eta_{\text{CA}}$ as discussed in Sec. IV. However, in the present microscopic model, the conductivity $\alpha = k_B \mu \lambda$ depends on λ . From Eq. (51) with $C = k_B/2$ and $\gamma = 1$, the power is given by

$$P = \frac{k_B \eta [(1 - \eta) T_h - T_c] \sinh(\mu(1 - \eta) \lambda_h \tau_c) \sinh(\mu \lambda_h \tau_h)}{(1 - \eta)(\tau_h + \tau_c) \sinh(\mu(1 - \eta) \lambda_h \tau_c + \mu \lambda_h \tau_h)}. \quad (75)$$

Here, the power is a function of the parameter λ_h , the efficiency, and the durations for given T_h , T_c , and μ , i.e., $P = P(\lambda_h, \eta, \tau_h, \tau_c; T_h, T_c, \mu)$. Since P depends on λ_h and λ_c with the ratio $\lambda_c/\lambda_h = 1 - \eta$, we should optimize both λ_h and η for the fully optimized case. However, as shown later, the power increases with λ_h so that, if we optimize λ_h , the maximum power diverges at infinite λ_h . Since λ is finite and can be easily fixed in experiments, the case with optimized η for given λ_h is more useful compared to the fully optimized case.

To get the efficiency at maximum power under given τ , λ_h , T_h , T_c , and μ , we optimize η , τ_h , and τ_c with the constraint,

$$\tau = \tau_h + \tau_c, \quad (76)$$

using the Lagrange multiplier method. With a Lagrange multiplier ξ , we define a function P' as

$$P'(\eta, \tau_h, \tau_c) \equiv P(\eta, \tau_h, \tau_c) - \xi \cdot (\tau_h + \tau_c). \quad (77)$$

For the maximum power, we have

$$\left(\frac{\partial P'}{\partial \eta} \right)_{\tau_h, \tau_c} = \left(\frac{\partial P'}{\partial \tau_h} \right)_{\eta, \tau_c} = \left(\frac{\partial P'}{\partial \tau_c} \right)_{\eta, \tau_h} = 0. \quad (78)$$

By eliminating ξ from the three equations of Eq. (78), we get

$$(1 - \eta) \sinh^2(\tau_h \mu \lambda_h) = \sinh^2[\tau_c (1 - \eta) \mu \lambda_h], \quad (79)$$

and

$$\frac{T_c}{T_h} - (1 - \eta)^2 + \frac{\eta[(1 - \eta) - \frac{T_c}{T_h}](1 - \eta) \mu \lambda_h \tau_c \sinh(\mu \lambda_h \tau_h)}{\sinh[(1 - \eta) \mu \lambda_h \tau_c] \sinh[(1 - \eta) \mu \lambda_h \tau_c + \mu \lambda_h \tau_h]} = 0. \quad (80)$$

The solution of the combined nonlinear equations (79) and (80) together with the constraint condition (76) gives η_{MP} and

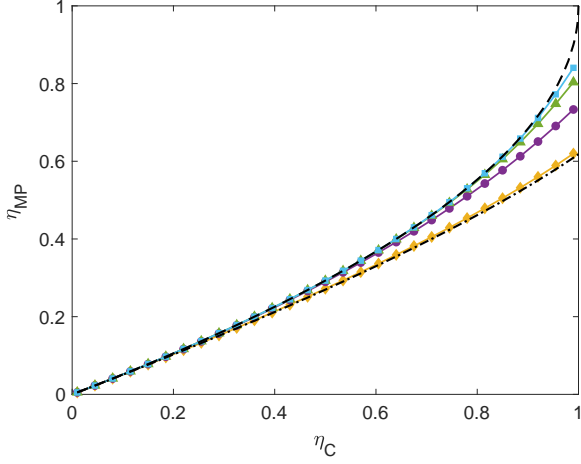


FIG. 4. η_{MP} as a function of η_C for various values of τ . In the limit of the large cycle period $\tau/(\mu\lambda_h)^{-1} \rightarrow \infty$, we have $\eta_{MP} = \eta_{CA}$ shown by the black dashed line. In the limit of the small cycle period $\tau/(\mu\lambda_h)^{-1} \rightarrow 0$, the resulting η_{MP} is shown by the black dashed-dotted line. The solid lines with symbols show η_{MP} for $\tau/(\mu\lambda_h)^{-1} = 1$ (yellow diamonds), 5 (purple circles), 9 (green triangles), and 13 (cyan squares).

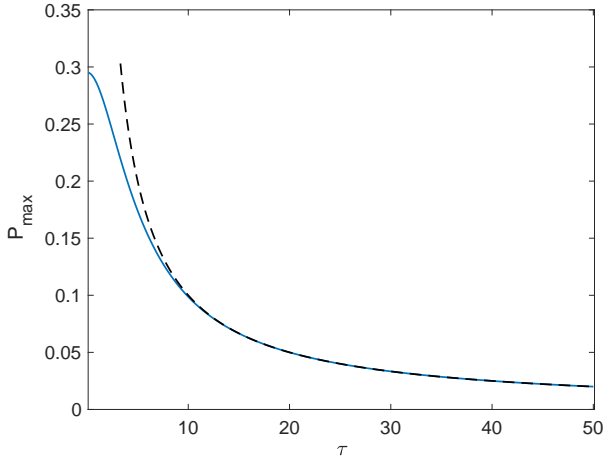


FIG. 5. P_{\max} as a function of τ . We set $T_c/T_h = 0.1$. P_{\max} is in units of $\mu\lambda_h k_B T_h \eta_{CA}^2/2$ and τ is in units of $(\mu\lambda_h)^{-1}$. The dashed line shows $1/\tau$.

optimized durations τ_h^* and τ_c^* for given τ . Note that, in these equations, $\mu\lambda_h$ always appears in the form of $\mu\lambda_h \tau_i$ for $i = h$ and c . We thus define new variables $\tilde{\tau}_i = \mu\lambda_h \tau_i$. Then the solutions η_{MP} and $\tilde{\tau}_i^*$ depend only on the cycle period τ and the temperature ratio $T_c/T_h = 1 - \eta_C$. Figure 4 shows the deviation of η_{MP} from η_{CA} for given values of τ .

Substituting η_{MP} , $\tilde{\tau}_h^*$, and $\tilde{\tau}_c^*$ into Eq. (75), we get the maximum power $P_{\max}(\tau)$ as a function of the cycle period τ which is in the form of

$$P_{\max}(\tau) = \mu\lambda_h k_B T_h f(\tau; T_c/T_h) \quad (81)$$

with given $\mu\lambda_h$, T_h , and T_c . Here, $f(\tau; T_c/T_h)$ is a dimension-

less function. Figure 5 shows the numerical result of $P_{\max}(\tau)$. Note that $P_{\max}(\tau)$ is maximized when the cycle period τ approaches zero. To get a physical understanding, let us consider the mean value of work in the \mathcal{P} - λ plane, where \mathcal{P} is the generalized pressure defined as $\mathcal{P} = \langle \partial H / \partial \lambda \rangle = \sigma_x / 2$. Then, as can be seen from Fig. 3, the mean value of the work output through one cycle is given by $\langle W \rangle = \Delta\lambda \Delta\sigma_x / 2$. Thus, the power is proportional to the changing rate of σ_x : $P \propto \Delta\sigma_x / \tau$. According to Eqs. (59) and (68), the changing rate $\dot{\sigma}_x$ is proportional to the temperature difference $T - \tilde{T}$ between the working substance and the bath. Since the temperature difference is finite and takes a maximum value at the beginning of each heat transfer stroke, $\dot{\sigma}_x$ is finite and maximized when $\tau \rightarrow 0$. Therefore, the power is also finite and maximized at $\tau \rightarrow 0$.

As can be seen from Fig. 4, the value of η_{MP} increases as the cycle period and is between the black dashed line and the black dashed-dotted line. Here, the black dashed (dashed-dotted) line shows η_{MP} in the limit of large (small) cycle period. For large durations $\tau_h \gg (\mu\lambda_h)^{-1}$ and $\tau_c \gg (\mu\lambda_c)^{-1}$, the third term in the LHS of Eq. (80) is negligible. Thus, we get

$$\eta_{MP} = 1 - \sqrt{\frac{T_c}{T_h}} = \eta_{CA} \quad (82)$$

from Eq. (80), and

$$P_{\max} = k_B T_h \eta_{CA}^2 / (2\tau) \quad (83)$$

from Eq. (75).

For small cycle period $\tau \ll (\mu\lambda_h)^{-1}$, we have $\sinh \tau_i \simeq \tau_i$, and Eqs. (79) and (80) become

$$\eta_{MP} = 1 - \frac{\tau_h^2}{\tau_c^2} \quad (84)$$

and

$$(2\eta_{MP} - \eta_C) \tau_h = [\eta_{MP}^2 - 2\eta_{MP} + \eta_C] \tau_c, \quad (85)$$

respectively. Substituting Eq. (84) into Eq. (85), we get

$$\eta_{MP}(1 + \sqrt{1 - \eta_{MP}}) = \eta_C. \quad (86)$$

From Eqs. (84) and (86), the maximum power given by Eq. (75) becomes

$$P_{\max} = \mu\lambda_h k_B T_h (\eta_C - \eta_{MP}) \eta_{MP}^3 / \eta_C^2. \quad (87)$$

For $T_c/T_h \simeq 1$ so that $\eta_C \ll 1$, from Eq. (86) we can expand η_{MP} as

$$\eta_{MP} = \frac{1}{2}\eta_C + \frac{1}{16}\eta_C^2 + \frac{3}{128}\eta_C^3 + O(\eta_C^4). \quad (88)$$

On the other hand, expanding the CA efficiency $\eta_{CA} = 1 - \sqrt{T_c/T_h}$ around $T_c/T_h = 1$, we obtain

$$\eta_{CA} = \frac{1}{2}\eta_C + \frac{1}{8}\eta_C^2 + \frac{3}{16}\eta_C^3 + O(\eta_C^4). \quad (89)$$

In conclusion, we have

$$\eta_{MP} \lesssim \eta_{CA} \quad (90)$$

for the endoreversible small Otto engine. Here, η_{MP} approaches η_{CA} as the cycle period increases or η_C decreases.

2. Ratio $\eta_{\text{MP}}^{(2)}$ at maximum power

Since there is no work output during the heat transfer strokes in the Otto cycle, work and heat are determined solely by the energy change in each stroke:

$$W = \frac{1}{2}(\lambda_h - \lambda_c)[x(\tau_h)^2 - x(0)^2] \quad (91)$$

and

$$Q_h = \frac{1}{2}\lambda_h[x(\tau_h)^2 - x(0)^2]. \quad (92)$$

Therefore, the stochastic efficiency $\tilde{\eta} \equiv W/Q_h = 1 - \lambda_c/\lambda_h$ becomes deterministic and agrees with the efficiency $\eta = \langle W \rangle / \langle Q_h \rangle = 1 - \lambda_c/\lambda_h$. In addition, $\eta^{(2)} \equiv \langle (\Delta W)^2 \rangle / \langle (\Delta Q_h)^2 \rangle$ becomes

$$\eta^{(2)} = \left(1 - \frac{\lambda_c}{\lambda_h}\right)^2 = \eta^2. \quad (93)$$

It is noted that the relations $\eta = 1 - (\lambda_c/\lambda_h) < \eta_C$ and $\eta^{(2)} = \eta^2 < \eta_C^2$ hold for any cycle period within the Otto engine. Thus, from Eqs. (90) and (93), we have

$$\eta_{\text{MP}}^{(2)} = \eta_{\text{MP}}^2 \lesssim \eta_{\text{CA}}^2. \quad (94)$$

In addition, since $\eta_{\text{CA}} \leq \eta_C$, η_C^2 is still the upper bound of $\eta_{\text{MP}}^{(2)}$ for the endoreversible small Otto engine.

3. Cumulant of work

The higher order cumulants $\langle W^n \rangle_c$ of work output can be calculated analytically from Eq. (66). Note that the higher order cumulants generally depend on the starting point of the cycle [66]. For the Otto cycle, the n th order cumulant of work output is given by

$$\langle W^n \rangle_c = \frac{(n-1)!}{2} \left[(1-c)a^n + (1-c)b^n + c(a+b)^n \right] \quad (95)$$

with $a = (\lambda_h - \lambda_c)\sigma_x(\tau_h)$, $b = (\lambda_c - \lambda_h)\sigma_x(0)$, and $c = \phi(\tau_h, \tau) / [\sigma_x(0)\sigma_x(\tau_h)]$ when starting just before the adiabatic expansion; with $a = (\lambda_c - \lambda_h)\sigma_x(0)$, $b = (\lambda_h - \lambda_c)\sigma_x(\tau_h)$, and $c = \phi(0, \tau_h) / [\sigma_x(0)\sigma_x(\tau_h)]$ when starting just before the adiabatic compression. For some special cases, we can get an analytical expression of the PDF of work $P(W)$. For example, when $a + b = 0$, we have

$$P(W) = \frac{K_0(|W/a|)}{\pi|a|}, \quad (96)$$

where $K_0(x)$ is the zeroth order modified Bessel function of the second kind. In addition, for the heat input $Q_h = W/\eta$, all the cumulants are given by $\langle Q_h^n \rangle_c = \eta^{-n} \langle W^n \rangle_c$. The PDFs of work and heat given by the modified Bessel function have been obtained also in other similar systems [67–74].

B. Brownian Curzon-Ahlborn heat engine

For the small Curzon-Ahlborn heat engine, we assume that the working substance follows the Carnot cycle which consists of two adiabatic jumps and two isothermal strokes. Suppose we have the adiabatic expansion (compression) at $t = \tau_h$ ($t = 0$) and the cycle period $\tau = \tau_c + \tau_h$. During the hot (cold) isothermal strokes, both the water temperature T_h (T_c) and the effective temperature of the working substance \tilde{T}_h (\tilde{T}_c) are constant. As a consequence, $\dot{\sigma}_x = 2\mu k_B(T_i - \tilde{T}_i)$ with $i = h, c$ given by Eq. (59) is constant. Thus, the effective temperatures \tilde{T}_h and \tilde{T}_c are given by

$$\tilde{T}_h = T_h - \frac{\sigma_x(\tau_h) - \sigma_x(0)}{2\mu k_B \tau_h}, \quad (97)$$

$$\tilde{T}_c = T_c + \frac{\sigma_x(\tau_h) - \sigma_x(0)}{2\mu k_B \tau_c}. \quad (98)$$

From the Newton law (73), the thermal conductivity is given by $\alpha_i = \mu \tilde{T}_i [\ln \sigma_x(\tau_h) - \ln \sigma_x(0)] / [\sigma_x(\tau_h) - \sigma_x(0)]$. If the conductivity is constant, the efficiency at maximum power is the CA efficiency. However, here $\alpha_i(\tilde{T}_i; \sigma_x, \mu)$ is no longer constant, but depends on the effective temperature of the working substance.

1. Efficiency at maximum power

Now, we derive η_{MP} of the microscopic CA engine. The power is given by

$$\begin{aligned} P &\equiv \frac{\langle W \rangle}{\tau} \\ &= -\frac{1}{2\tau} \int \sigma_x d\lambda \\ &= -\frac{1}{2\tau} \int \sigma_x d\left(\frac{k_B \tilde{T}_i}{\sigma_x}\right) \\ &= \frac{k_B}{2\tau} (\tilde{T}_h - \tilde{T}_c) \ln \frac{\sigma_x(\tau_h)}{\sigma_x(0)} \\ &= \frac{k_B}{2} \ln \frac{\sigma_x(\tau_h)}{\sigma_x(0)} \left[\frac{T_h - T_c}{\tau_c + \tau_h} - \frac{\sigma_x(\tau_h) - \sigma_x(0)}{2\mu k_B \tau_c \tau_h} \right]. \end{aligned} \quad (99)$$

By maximizing the power with respect to τ_c and τ_h under given T_h , T_c , μ , $\sigma_x(0)$, and $\sigma_x(\tau_h)$, we get $\tau_c = \tau_h = \tau_{\text{MP}}/2$ with

$$\tau_{\text{MP}} = \frac{4[\sigma_x(\tau_h) - \sigma_x(0)]}{\mu k_B (T_h - T_c)}. \quad (100)$$

Substituting τ_{MP} into Eqs. (97) and (98), we get the effective temperatures: $\tilde{T}_h = (3/4)T_h + (1/4)T_c$ and $\tilde{T}_c = (1/4)T_h + (3/4)T_c$. Then η_{MP} is given by

$$\eta_{\text{MP}} = 1 - \frac{\tilde{T}_c}{\tilde{T}_h} = \frac{2(T_h - T_c)}{3T_h + T_c} = \frac{\eta_C}{2 - \eta_C/2}. \quad (101)$$

This result agrees with that of Ref. [52] for the finite-time Brownian heat engines at maximum power. As shown in Fig. 6, the approximate relation $\eta_{\text{MP}} \simeq \eta_{\text{CA}}$ holds when $\eta_C \ll 1$.

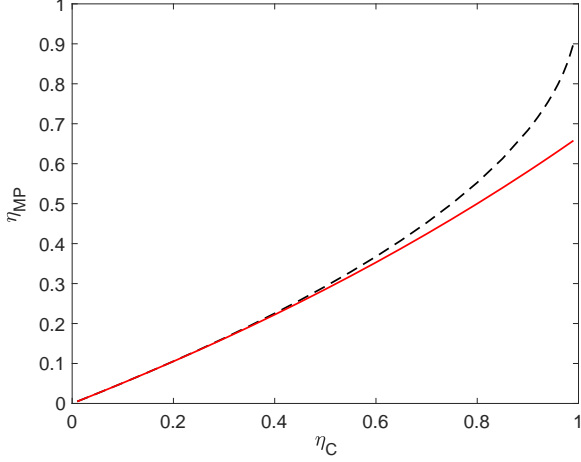


FIG. 6. η_{MP} for the microscopic CA engine as a function of η_C . The dashed line shows η_{CA} .

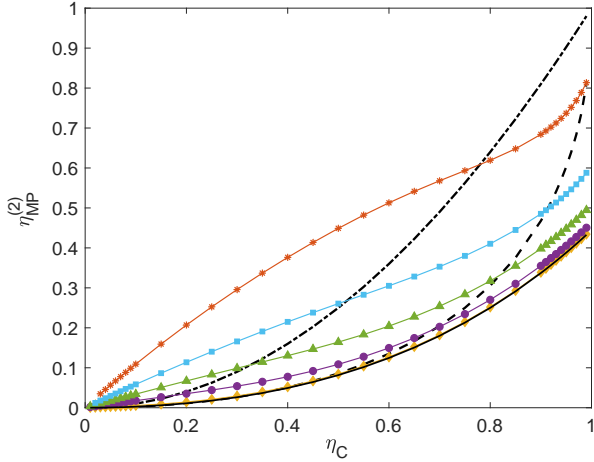


FIG. 7. $\eta_{\text{MP}}^{(2)}$ as a function of η_C for various values of $\sigma_x(0)/\sigma_x(\tau_h)$. Solid lines with symbols show $\eta_{\text{MP}}^{(2)}$ for $\sigma_x(0)/\sigma_x(\tau_h) = 0.1$ (orange asterisks), 0.3 (cyan squares), 0.5 (green triangles), 0.7 (purple circles), and 0.9 (yellow diamonds). The black dashed-dotted line shows η_C^2 , the black dashed line shows η_{CA}^2 , and the black solid line shows η_{MP}^2 with η_{MP} given by Eq. (101).

2. Ratio $\eta_{\text{MP}}^{(2)}$ at maximum power

Numerically, we find that $\eta_{\text{MP}}^{(2)}$ for the CA engine depends only on the ratio $\sigma_x(0)/\sigma_x(\tau_h)$ and η_C . As shown in Fig. 7, we have $\eta_{\text{MP}}^{(2)} \simeq \eta_{\text{MP}}^2$ for $\sigma_x(0)/\sigma_x(\tau_h) \simeq 1$. That is because when $\sigma_x(0) \simeq \sigma_x(\tau_h)$, $\lambda = k_B \bar{T}/\sigma_x$ is almost unchanged during the isothermal strokes. Then, the isothermal strokes become isochoric and the CA engine becomes identical to the Otto engine. In this case, work is extracted only in the reversible adiabatic strokes and we have $\eta_{\text{MP}}^{(2)} = \eta_{\text{MP}}^2$ as discussed in the example of the Otto engine. Since η_{MP} is close to η_{CA} for the CA engine, we have $\eta_{\text{MP}}^{(2)} \simeq \eta_{\text{CA}}^2$ when $\sigma_x(0)$ is close to $\sigma_x(\tau_h)$.

The situation here is very different from that in Sec. IV. In Sec. IV, we assume that the heat conductivities are constant, and the cycle period is sufficiently large such that the effect of the correlation of work is negligible. Here, from Eq. (100), we find that the condition $\sigma_x(0)/\sigma_x(\tau_h) \simeq 1$ gives a very small cycle period. Therefore, in the case of the CA engine, the approximate relation $\eta_{\text{MP}}^{(2)} \simeq \eta_{\text{CA}}^2$ holds even when the cycle period is small and the heat conductivities are not constant.

In addition, the relation $\eta_{\text{MP}}^{(2)} \simeq \eta_{\text{CA}}^2 < \eta_C^2$ also indicates that the upper bound η_C^2 is still applicable to the CA engine with $\sigma_x(0)/\sigma_x(\tau_h) \simeq 1$. However, as shown in Fig. 7, $\eta_{\text{MP}}^{(2)}$ could exceed η_C^2 for the CA engine with small η_C and small $\sigma_x(0)/\sigma_x(\tau_h)$.

VII. SUMMARY AND CONCLUSION

In summary, we have studied the ratio between the variances of work output and heat input, $\eta^{(2)}$, for endoreversible small heat engines. We have found that the ratio $\eta_{\text{MP}}^{(2)}$ at maximum power is equal or close to the square of the Curzon-Ahlborn (CA) efficiency, $\eta_{\text{MP}}^{(2)} \simeq \eta_{\text{CA}}^2$, for endoreversible small heat engines.

Endoreversible small heat engines have the working substance following a reversible cycle and the finite irreversible heat flow causing the finite-time effect. Thus, we separated our discussion into two parts: (i) we first considered $\eta^{(2)}$ for reversible small heat engines in the quasistatic limit in Sec. III, and (ii) we discussed the ratio $\eta_{\text{MP}}^{(2)}$ at maximum power for the endoreversible small heat engines in Sec. IV. We considered a class of four-stroke heat engines operating with two heat baths with the temperatures T_h and T_c consisting of two adiabatic strokes and two heat transfer strokes with constant heat capacities C_h and C_c . In part (i), the ratio $\theta = C_h/C_c$ is crucial for the relation between $\eta^{(2)}$ and η^2 . (a) For $\theta < 1$, η^2 gives a lower bound of $\eta^{(2)}$; (b) for $\theta > 1$, η^2 does not give the lower bound of $\eta^{(2)}$ any more, and $\eta^{(2)}$ could be larger or smaller than η^2 ; (c) in the typical case of $\theta = 1$ (e.g., the Otto cycle, the Brayton cycle, and the Carnot cycle), we obtained $\eta^{(2)} = \eta^2$. In part (ii), we considered the typical case of $\theta = 1$. We assumed the heat transfer following the Fourier law or the Newton law. For the constant heat conductivities, when the cycle period is much larger than the correlation time of work and heat, we obtained $\eta_{\text{MP}}^{(2)} = \eta_{\text{MP}}^2 = \eta_{\text{CA}}^2 = (1 - \sqrt{T_c/T_h})^2$ in Sec. IV. Then, in the last two sections (Secs. V and VI), we have verified that η_{CA}^2 gives a good estimate of $\eta_{\text{MP}}^{(2)}$, i.e., $\eta_{\text{MP}}^{(2)} \simeq \eta_{\text{CA}}^2$, for the endoreversible Brownian heat engines. In Sec. V, we introduced the endoreversible Brownian heat engine and gave an expression of the cumulant of work and heat. In Sec. VI, by taking the two type of the Brownian heat engine cycle as examples, we have shown that the approximate relation $\eta_{\text{MP}}^{(2)} \simeq \eta_{\text{CA}}^2$ holds even when the cycle period is smaller than the correlation time of work and heat and the heat conductivities are not constant. We discussed (a) the Brownian Otto engine in Sec. VIA and (b) the Brownian CA engine in

Sec. **VIB**. (a) For the Otto engine, since $\eta^{(2)} = \eta^2$ ($\eta \leq \eta_C$) always holds and η_{MP} is close to η_{CA} , we have $\eta_{MP}^{(2)} \simeq \eta_{CA}^2$. (b) For the CA engine, we have found that $\eta_{MP}^{(2)} \simeq \eta_{CA}^2$ holds when the work in the isothermal strokes is small. In this case, the CA engine is close to the Otto engine, and the work is mostly done through the reversible adiabatic strokes. In addition, since $\eta_{CA}^2 \leq \eta_C^2$, the upper bound of $\eta^{(2)}$ in the quasistatic limit, η_C^2 , is applicable to some endoreversible small heat engines at maximum power when the relation $\eta_{MP}^{(2)} \simeq \eta_{CA}^2$ holds.

Our result, $\eta_{MP}^{(2)} \simeq \eta_{CA}^2$, resembles the relation $\eta_{MP} \simeq \eta_{CA}$, i.e., as the CA efficiency gives a good estimate of the efficiency at maximum power for various kinds of finite-time heat engines, η_{CA}^2 also gives a good estimate of $\eta_{MP}^{(2)}$ for various finite-time small heat engines. Since the smaller $\eta^{(2)}$ means more stable work output converted from the fluctuat-

ing heat input, $\eta_{MP}^{(2)} \simeq \eta_{CA}^2$ also suggests a trade-off between the efficiency and the stability of finite-time heat engines at maximum power. In the future, finding an upper and a lower bound of $\eta_{MP}^{(2)}$ and minimizing the fluctuation of work output for the finite-time heat engines are interesting open problems. Also, thermodynamic geometry [25, 26, 58, 75–78] is a good method which leads to further studies on the properties of $\eta^{(2)}$.

ACKNOWLEDGEMENT

We thank Kosuke Ito for helpful discussions and comments. G. W. is supported by NSF of China (Grant No. 11975199), by the Zhejiang Provincial Natural Science Foundation Key Project (Grant No. LZ19A050001).

-
- [1] T. Hugel, N. B. Holland, A. Cattani, L. Moroder, M. Seitz, and H. E. Gaub, Single-Molecule Optomechanical Cycle, *Science* **296**, 1103 (2002).
- [2] P. G. Steeneken, K. Le Phan, M. J. Goossens, G. E. J. Koops, G. J. A. M. Brom, C. van der Avoort, and J. T. M. van Beek, Piezoresistive heat engine and refrigerator, *Nat. Phys.* **7**, 354 (2011).
- [3] S. Toyabe, T. Sagawa, M. Ueda, E. Muneyuki, and M. Sano, Experimental demonstration of information-to-energy conversion and validation of the generalized Jarzynski equality, *Nat. Phys.* **6**, 988 (2010).
- [4] V. Blickle and C. Bechinger, Realization of a micrometre-sized stochastic heat engine, *Nat. Phys.* **8**, 143 (2012).
- [5] I. A. Martínez, É. Roldán, L. Dinis, D. Petrov, J. M. R. Parrondo, and R. A. Rica, Brownian Carnot engine, *Nat. Phys.* **12**, 67 (2016).
- [6] S. Krishnamurthy, S. Ghosh, D. Chatterji, R. Ganapathy, and A. K. Sood, A micrometre-sized heat engine operating between bacterial reservoirs, *Nat. Phys.* **12**, 1134 (2016).
- [7] A. Argun, J. Soni, L. Dabelow, S. Bo, G. Pesce, R. Eichhorn, and G. Volpe, Experimental realization of a minimal microscopic heat engine, *Phys. Rev. E* **96**, 052106 (2017).
- [8] I. A. Martínez, É. Roldán, L. Dinis, and R. A. Rica, Colloidal heat engines: a review, *Soft Matter* **13**, 22 (2017).
- [9] S. Ciliberto, Experiments in Stochastic Thermodynamics: Short History and Perspectives, *Phys. Rev. X* **7**, 021051 (2017).
- [10] S. Erbas-Cakmak, D. A. Leigh, C. T. McTernan, and A. L. Nussbaumer, Artificial Molecular Machines, *Chem. Rev.* **115**, 10081 (2015).
- [11] K. Sekimoto, *Stochastic Energetics* (Springer, Berlin, Heidelberg, 2010).
- [12] U. Seifert, Stochastic thermodynamics, fluctuation theorems and molecular machines, *Rep. Prog. Phys.* **75**, 126001 (2012).
- [13] U. Seifert, From Stochastic Thermodynamics to Thermodynamic Inference, *Annu. Rev. Condens. Matter Phys.* **10**, 171 (2019).
- [14] C. Jarzynski, Equalities and Inequalities: Irreversibility and the Second Law of Thermodynamics at the Nanoscale, *Annu. Rev. Condens. Matter Phys.* **2**, 329 (2011).
- [15] C. Bustamante, J. Liphardt, and F. Ritort, The Nonequilibrium Thermodynamics of Small Systems, *Phys. Today* **58**, 43 (2005).
- [16] S. Ciliberto, S. Joubaud, and A. Petrosyan, Fluctuations in out-of-equilibrium systems: from theory to experiment, *J. Stat. Mech.* **2010**, P12003 (2010).
- [17] N. A. Sinitsyn, Fluctuation relation for heat engines, *J. Phys. A: Math. Theor.* **44**, 405001 (2011).
- [18] S. Lahiri, S. Rana, and A. M. Jayannavar, Fluctuation relations for heat engines in time-periodic steady states, *J. Phys. A: Math. Theor.* **45**, 465001 (2012).
- [19] M. Campisi, Fluctuation relation for quantum heat engines and refrigerators, *J. Phys. A: Math. Theor.* **47**, 245001 (2014).
- [20] S. Rana, P. S. Pal, A. Saha, and A. M. Jayannavar, Single-particle stochastic heat engine, *Phys. Rev. E* **90**, 042146 (2014).
- [21] Y. Zheng and D. Poletti, Work and efficiency of quantum Otto cycles in power-law trapping potentials, *Phys. Rev. E* **90**, 012145 (2014).
- [22] K. Ito, C. Jiang, and G. Watanabe, Universal Bounds for Fluctuations in Small Heat Engines (2019), [arXiv:1910.08096 \[cond-mat.stat-mech\]](https://arxiv.org/abs/1910.08096).
- [23] S. Saryal and B. K. Agarwalla, Bounds on fluctuations for finite-time quantum Otto cycle, *Phys. Rev. E* **103**, L060103 (2021).
- [24] S. Saryal, S. Mohanta, and B. K. Agarwalla, Bounds on fluctuations for machines with broken time-reversal symmetry: A linear response study, *Phys. Rev. E* **105**, 024129 (2022).
- [25] H. J. D. Miller and M. Mehboudi, Geometry of Work Fluctuations versus Efficiency in Microscopic Thermal Machines, *Phys. Rev. Lett.* **125**, 260602 (2020).
- [26] G. Watanabe and Y. Minami, Finite-time thermodynamics of fluctuations in microscopic heat engines, *Phys. Rev. Research* **4**, L012008 (2022).
- [27] V. Holubec and A. Ryabov, Fluctuations in heat engines, *J. Phys. A: Math. Theor.* **55**, 013001 (2021).
- [28] Y. H. Chen, J.-F. Chen, Z. Fei, and H. T. Quan, Microscopic theory of the Curzon-Ahlborn heat engine based on a Brownian particle, *Phys. Rev. E* **106**, 024105 (2022).
- [29] C. Kwon, J. D. Noh, and H. Park, Work fluctuations in a time-dependent harmonic potential: Rigorous results beyond the overdamped limit, *Phys. Rev. E* **88**, 062102 (2013).

- [30] D. S. P. Salazar, Work distribution in thermal processes, *Phys. Rev. E* **101**, 030101(R) (2020).
- [31] G. Verley, M. Esposito, T. Willaert, and C. Van den Broeck, The unlikely Carnot efficiency, *Nat. Commun.* **5**, 4721 (2014).
- [32] G. Verley, T. Willaert, C. Van den Broeck, and M. Esposito, Universal theory of efficiency fluctuations, *Phys. Rev. E* **90**, 052145 (2014).
- [33] M. Poletti, G. Verley, and M. Esposito, Efficiency Statistics at All Times: Carnot Limit at Finite Power, *Phys. Rev. Lett.* **114**, 050601 (2015).
- [34] J.-H. Jiang, B. K. Agarwalla, and D. Segal, Efficiency Statistics and Bounds for Systems with Broken Time-Reversal Symmetry, *Phys. Rev. Lett.* **115**, 040601 (2015).
- [35] K. Proesmans, B. Cleuren, and C. Van den Broeck, Stochastic efficiency for effusion as a thermal engine, *EPL* **109**, 20004 (2015).
- [36] L. P. Fischer, P. Pietzonka, and U. Seifert, Large deviation function for a driven underdamped particle in a periodic potential, *Phys. Rev. E* **97**, 022143 (2018).
- [37] S. K. Manikandan, L. Dabelow, R. Eichhorn, and S. Krishnamurthy, Efficiency Fluctuations in Microscopic Machines, *Phys. Rev. Lett.* **122**, 140601 (2019).
- [38] A. C. Barato and U. Seifert, Thermodynamic Uncertainty Relation for Biomolecular Processes, *Phys. Rev. Lett.* **114**, 158101 (2015).
- [39] T. R. Gingrich, J. M. Horowitz, N. Perunov, and J. L. England, Dissipation Bounds All Steady-State Current Fluctuations, *Phys. Rev. Lett.* **116**, 120601 (2016).
- [40] J. Horowitz and T. Gingrich, Thermodynamic uncertainty relations constrain non-equilibrium fluctuations, *Nat. Phys.* **16**, 15 (2020).
- [41] P. Pietzonka and U. Seifert, Universal Trade-Off between Power, Efficiency, and Constancy in Steady-State Heat Engines, *Phys. Rev. Lett.* **120**, 190602 (2018).
- [42] V. Holubec and A. Ryabov, Cycling Tames Power Fluctuations near Optimum Efficiency, *Phys. Rev. Lett.* **121**, 120601 (2018).
- [43] A. C. Barato, R. Chetrite, A. Faggionato, and D. Gabrielli, Bounds on current fluctuations in periodically driven systems, *New J. Phys.* **20**, 103023 (2018).
- [44] T. Koyuk, U. Seifert, and P. Pietzonka, A generalization of the thermodynamic uncertainty relation to periodically driven systems, *J. Phys. A: Math. Theor.* **52**, 02LT02 (2018).
- [45] T. Koyuk and U. Seifert, Operationally Accessible Bounds on Fluctuations and Entropy Production in Periodically Driven Systems, *Phys. Rev. Lett.* **122**, 230601 (2019).
- [46] S. Saryal, M. Gerry, I. Khait, D. Segal, and B. K. Agarwalla, Universal Bounds on Fluctuations in Continuous Thermal Machines, *Phys. Rev. Lett.* **127**, 190603 (2021).
- [47] I. I. Novikov, The efficiency of atomic power stations (a review), *J. Nucl. Energy* (1954) **7**, 125 (1958).
- [48] F. L. Curzon and B. Ahlborn, Efficiency of a Carnot engine at maximum power output, *Am. J. Phys.* **43**, 22 (1975).
- [49] K. Hoffmann, J. Burzler, and S. Schubert, Endoreversible Thermodynamics, *J. Non-Equilib. Thermodyn.* **22**, 311 (1997).
- [50] B. Andresen, Current Trends in Finite-Time Thermodynamics, *Angew. Chem. Int. Ed.* **50**, 2690 (2011).
- [51] Q. Bouton, J. Nettersheim, S. Burgardt, D. Adam, E. Lutz, and A. Widera, A quantum heat engine driven by atomic collisions, *Nat. Commun.* **12**, 2063 (2021).
- [52] T. Schmiedl and U. Seifert, Efficiency at maximum power: An analytically solvable model for stochastic heat engines, *EPL* **81**, 20003 (2007).
- [53] A. Dechant, N. Kiesel, and E. Lutz, All-Optical Nanomechanical Heat Engine, *Phys. Rev. Lett.* **114**, 183602 (2015).
- [54] A. Dechant, N. Kiesel, and E. Lutz, Underdamped stochastic heat engine at maximum efficiency, *EPL* **119**, 50003 (2017).
- [55] S. Deffner, Efficiency of Harmonic Quantum Otto Engines at Maximal Power, *Entropy* **20**, 875 (2018).
- [56] J.-F. Chen, C.-P. Sun, and H. Dong, Achieve higher efficiency at maximum power with finite-time quantum Otto cycle, *Phys. Rev. E* **100**, 062140 (2019).
- [57] J.-F. Chen, C.-P. Sun, and H. Dong, Boosting the performance of quantum Otto heat engines, *Phys. Rev. E* **100**, 032144 (2019).
- [58] Y. Izumida, Irreversible efficiency and Carnot theorem for heat engines operating with multiple heat baths in linear response regime, *Phys. Rev. Research* **4**, 023217 (2022).
- [59] P. T. Landsberg and H. S. Leff, Thermodynamic cycles with nearly universal maximum-work efficiencies, *J. Phys. A: Math. Gen.* **22**, 4019 (1989).
- [60] The term “reversible” in this work means that the working substance of the engine is reversible such that the working substance is always in a canonical state for some temperature. Following the assumption of endoreversible thermodynamics, we regard that the working substance is reversible, but the heat flow between the working substance and the bath can be irreversible.
- [61] There are many cases that the heat capacities of the heat transfer strokes are constant. For example, isobaric and isochoric strokes for a Brownian particle in a harmonic oscillator potential or a square-well potential.
- [62] K. Sato, K. Sekimoto, T. Hondou, and F. Takagi, Irreversibility resulting from contact with a heat bath caused by the finiteness of the system, *Phys. Rev. E* **66**, 016119 (2002).
- [63] H. Qian, Mesoscopic nonequilibrium thermodynamics of single macromolecules and dynamic entropy-energy compensation, *Phys. Rev. E* **65**, 016102 (2001).
- [64] The Hamiltonian in Ref. [42] is $H = kx^{2n}/2n$, where x is the position of the Brownian particle, k is the stiffness of the potential, and n is a natural number. In this case, C_V is constant, $C_V = k_B/(2n)$, which is in accordance with the assumption of our analysis. Therefore, Eq. (28) is applicable to this case, and gives $\sqrt{\sigma_W} = k_B/(\sqrt{n}\Delta S)$, which agrees with the result in Ref. [42].
- [65] C. W. Gardiner, *Handbook of Stochastic Methods*, 3rd ed. (Springer, Berlin, 2004).
- [66] G.-H. Xu and G. Watanabe, Correlation-enhanced stability of microscopic cyclic heat engines, *Phys. Rev. Research* **4**, L032017 (2022).
- [67] A. Imparato, L. Peliti, G. Pesce, G. Rusciano, and A. Sasso, Work and heat probability distribution of an optically driven Brownian particle: Theory and experiments, *Phys. Rev. E* **76**, 050101(R) (2007).
- [68] D. Chatterjee and B. J. Cherayil, Exact path-integral evaluation of the heat distribution function of a trapped Brownian oscillator, *Phys. Rev. E* **82**, 051104 (2010).
- [69] J. R. Gomez-Solano, A. Petrosyan, and S. Ciliberto, Heat Fluctuations in a Nonequilibrium Bath, *Phys. Rev. Lett.* **106**, 200602 (2011).
- [70] A. Pal and S. Sabhapandit, Work fluctuations for a Brownian particle in a harmonic trap with fluctuating locations, *Phys. Rev. E* **87**, 022138 (2013).
- [71] D. S. P. Salazar and S. A. Lira, Exactly solvable nonequilibrium Langevin relaxation of a trapped nanoparticle, *J. Phys. A: Math. Theor.* **49**, 465001 (2016).
- [72] A. Crisanti, A. Sarracino, and M. Zannetti, Heat fluctuations of Brownian oscillators in nonstationary processes: Fluctuation theorem and condensation transition, *Phys. Rev. E* **95**, 052138 (2017).

- [73] K. Goswami, Heat fluctuation of a harmonically trapped particle in an active bath, [Phys. Rev. E **99**, 012112 \(2019\)](#).
- [74] P. Chvosta, D. Lips, V. Holubec, A. Ryabov, and P. Maass, Statistics of work performed by optical tweezers with general time-variation of their stiffness, [J. Phys. A: Math. Theor. **53**, 275001 \(2020\)](#).
- [75] G. E. Crooks, Measuring Thermodynamic Length, [Phys. Rev. Lett. **99**, 100602 \(2007\)](#).
- [76] T. Van Vu and Y. Hasegawa, Geometrical bounds of the irreversibility in markovian systems, [Phys. Rev. Lett. **126**, 010601 \(2021\)](#).
- [77] K. Brandner and K. Saito, Thermodynamic Geometry of Microscopic Heat Engines, [Phys. Rev. Lett. **124**, 040602 \(2020\)](#).
- [78] A. G. Frim and M. R. DeWeese, Optimal finite-time Brownian Carnot engine, [Phys. Rev. E **105**, L052103 \(2022\)](#).